Phage-mediated dispersal of multicellular bacteria

Hoda Jaffal, Mounia Kortebi, Pauline Misson, Paulo Tavares, Malika Ouldali, Hervé Leh, Sylvie Lautru, Virginia S Lioy, François Lecointe, Stéphanie Bury-Moné

Phage-mediated dispersal of multicellular bacteria

Hoda Jaffal[a], Mounia Kortebi[a], Pauline Misson[b*], Paulo Tavares[a], Malika Ouldali[a], Hervé Leh[a], Sylvie Lautru[a], Virginia S. Lioy[a], François Lecointe[b], Stéphanie Bury-Moné[a#]

[a]Université Paris-Saclay, CEA, CNRS, Institute for Integrative Biology of the Cell (I2BC), 91198, Gif-sur-Yvette, France

[b]Université Paris-Saclay, INRAE, AgroParisTech, Micalis Institute, Jouy-en-Josas, France

[#]Address correspondence to Stéphanie Bury-Moné, stephanie.bury-mone@i2bc.paris-saclay.fr

[*]Present addresses: Medical Research Council London Institute of Medical Sciences, London, United Kingdom; Institute of Clinical Sciences, Faculty of Medicine, Imperial College London, London, United Kingdom

Running title: Phage-mediated dispersal of multicellular bacteria

ABSTRACT

Streptomyces are renowned for their prolific production of specialized metabolites with applications in medicine and agriculture. These multicellular bacteria present a sophisticated developmental cycle, and play a key role in soil ecology. Little is known about *Streptomyces*-phage interactions and the impact of phages on *Streptomyces* physiology. In this study, we investigated the conditions governing the expression and production of 'Samy', a prophage found in *Streptomyces ambofaciens* ATCC 23877. This phage is a siphovirus produced simultaneously with the activation of other mobile genetic elements. We show that Samy production increases bacterial dispersal in stress conditions, facilitating the dissemination of the lineage. Altogether, we unveiled a new property of a bacteriophage infection that it is closely linked to the multicellular community life of *Streptomyces* bacteria.

TEXT

INTRODUCTION

Streptomyces are among the most prolific producers of specialized metabolites, with applications in medicine and agriculture (1,2). These filamentous Gram-positive bacteria are widely distributed in the environment and play a key role in soil ecology (3,4). *Streptomyces* are a rare example of multicellular bacteria capable of forming hyphae with connected compartments. They present a complex life cycle that involves uni- to multi-cellular transitions, sporulation, metabolic differentiation, programmed cell death and exploration (3,5).

While *Streptomyces* is the largest prokaryotic genus with over 900 species (Genome Taxonomy Database, Release 08-RS214), relatively few *Streptomyces* phages have been characterized to date. They represent less than 2.5% of the bacterial viruses listed by the ICTV (Release 21-221122_MSL37) or the NCBI, and only 7.5 % of the Actinobacteriophage Database (6). The identified *Streptomyces* phages are double stranded DNA viruses (Caudovirales and *Tectiviridae*), with the possible exception of an RNA virus detected in a *Streptomyces* transcriptome (7). Nevertheless, research on phage diversity and impact on *Streptomyces* physiology and ecology is still in its infancy, with only a few examples to date (8).

By causing lysis of their host, some *Streptomyces* phages are likely to contribute to the death process of a part of the colony and/or to premature termination of antibiotic production. Accordingly, they can lead to industrial fermentation failure (9). Moreover, some phages may induce the release of specialized metabolites (10,11). Reciprocally, some bioactive compounds produced by *Streptomyces* can act as anti-phage defenses (12–14). Furthermore, some *Streptomyces* phages encode WhiB or Lsr2-type regulators (15). WhiB and Lsr2 are xenogeneic silencers that regulate sporulation and antibiotic production, respectively. Their phage homologs may possibly modulate these key steps of the *Streptomyces* life cycle. A recent study nicely illustrates that phage infection can impact the developmental cycle of *Streptomyces* (11). Reciprocally, susceptibility to phage infection varies along the developmental cycle (11,16). Altogether this illustrates how the study of *Streptomyces* - phage interplay can uncover new types of interactions based on specific traits of the complex life cycle of these bacteria.

The last few years have been marked by a sustained effort in the isolation and sequencing of *Streptomyces* phages from environmental samples (17–19,10,20,21). Moreover, the *Streptomyces* genome can constitute *per se* a viral genetic reservoir, through

the genomes of temperate prophages that they may host. Using PHASTER (22), prophage sequences were detected in all *Streptomyces* strains that were analyzed (*n* = 7) (23). The prophage state is, perhaps, one of the most important stages in the interaction between phage and host genomes. The lysogenic cycle represents an opportunity for phages to confer new properties to their host notably through the expression of moron genes that may contribute to bacterial fitness and environmental niche expansion (24).

In this study, we characterize a new temperate phage from *Streptomyces ambofaciens* ATCC 23877, which we named 'Samy'. This phage is produced under metabolic stress and activated at the same time as other mobile genetic elements. By exploring the impact of Samy activation on *Streptomyces* cell physiology, we observed bacterial dispersal in stress conditions. This type of dispersion mediated by phages was never reported in multicellular bacteria, but has been observed in multicellular-like environments of biofilms (25). This constitutes an emerging property associated with bacteriophage infection that is likely to enhance the spread of the species. Our study illustrates how prophages may play a role in the evolution and adaptability of *Streptomyces.*

MATERIALS AND METHODS

Streptomyces strains

The *Streptomyces* strains and primers used in this study are listed in supplementary **Table S1** and **Table S2**, respectively. A CRISPR-Cas9-based approach using a single guide RNA (SBM395, Supplementary **Table S2**) targeting the Samy integrase (SAMYPH_94/ SAM23877_RS39280) was conducted in the absence of a template donor DNA using pCRISPR-Cas9 vector, as previously described (26). The precise size of the deleted regions in 3 independent clones was determined by sequencing (Supplementary **Table S1**).

Growth conditions

All media composition are described in Supplementary **Table S3**. Bacteria were grown at 30°C. Spores were collected after growth on SFM medium. About 10^7 spores were inoculated in 50 mL of liquid medium (in a 500 mL Duran® Erlenmeyer baffled flask with a silicon stopper) and incubated in a shaking orbital agitator (200 rpm, INFORS Unitron standard). Aliquots from the cultures were collected, centrifuged and filtered using Whatman PVDF Mini-UniPrep syringeless filters (0.2 µm). Antibacterial activity against *Micrococcus luteus* was determined as previously described (27). The colony forming units (CFU) after 4 days of

growth in BM liquid medium were determined after serial dilutions in water, and plating of 100 µl of dilutions on SFM medium. To analyze the impact of conditioned supernatants on *S. ambofaciens* growth and survival, the WT strain or its isogenic mutant ΔSamy clone #3 were grown in BM medium during 24 h before supplementing the medium with filtered conditioned supernatants at ratios of 1:2 or 1:5 (supernatant: culture volume). Then, the bacteria were grown for an additional 3 days before counting.

Optical microscopy

After 4 days-growth in BM liquid medium, 10 µL of *Streptomyces* cultures were directly mounted on glass coverslips and analyzed using an Olympus BX63 microscope. Images were acquired with a 40x oil immersion objective.

Phage quantification by qPCR

Filtered supernatants were treated with 1U/100 µL TURBO DNAse (Invitrogen) for 1 h at 37°C, and then incubated for 20 min at 80°C. Amplification was carried out on 2 µL of these treated supernatants, in a final volume of 10 µL, using the LightCycler FastStart DNA Master HybProbe kit (Roche Diagnostics) supplemented with SYBR Green. Primers used to amplify Samy prophage and a host gene are indicated in Supplementary **Table S2**. The qPCR efficiencies as well as the absolute number of amplified copies were determined using 10^2 to 10^6 copies of *S. ambofaciens* ATCC 23877 gDNA as standard.

Infection assay

After 4 days-growth in BM liquid medium, *S. ambofaciens* ATCC 23877 culture was centrifuged at 8,000 rpm (JA14 rotor, Beckman) for 15 min at 4°C to pellet intact bacteria and debris. The supernatant was then transferred to new centrifuge tubes and subjected to overnight centrifugation under the same condition. The pellet was resuspended and serially diluted in TBT buffer (100 mM Tris-HCl, pH 7.5; 100 mM NaCl; 10 mM $MgCl_2$). Approximatively 10^8 spores of target bacteria [*Streptomyces albidoflavus* J1074, *S. ambofaciens* ATCC 23877, *S. ambofaciens* DSM 40497, *S. coelicolor* A3(2), *Streptomyces noursei* ATCC 11455, *Streptomyces rimosus* ATCC 10970, *Streptomyces venezuelae* ATCC 10712, Supplementary **Table S1**] were inoculated in 3 mL of SNA before pouring on SFM plates. Five µL of serial dilutions of the phage preparation were spotted on the bacterial lawns. The plates were incubated for one week before imaging.

Samy prophage detection and annotation

Synteruptor program (http://bim.i2bc.paris-saclay.fr/synteruptor/, v1.1) was used to compare the sequences of *S. ambofaciens* ATCC 23877 and *S. ambofaciens* DSM 40697 (27,28), with a minimal threshold of 20 CDSs to identify genomic islands. PHASTER (22) was used to predict the presence of a putative prophage in the *S. ambofaciens* chromosome. *In silico* translated Samy prophage CDSs predicted in *S. ambofaciens* ATCC 28377 chromosomal sequence [CP012382, initial annotation (29)] were functionally annotated using HHPred (30) against the PDB mmCIF70 (version of January 10, 2023) and PHROGs_V4 (31) databases. Functions (known or unknown) of the nearest homologs were transferred to the queries by only retaining predictions with a probability ≥ 95.8%. The genome comparison between Samy and PhiC31 was performed using Easyfig software (e-value $<10^{-3}$, v2.2.5). No significant similarity with a previously annotated CDS led to a 'hypothetical protein' annotation. In case of identification of a protein related to an annotated PHROG of unknown function, the annotation of the gene is 'protein of unknown function' with a note indicating the related-PHROG number. This first annotation was manually curated using the more recently submitted version of *S. ambofaciens* ATCC 28377 chromosome annotation (NZ_CP012382, released 2022-04-14). The annotated genes have an identifier starting with "SAMYPH".

RNA preparation, sequencing and data processing

About 2.10^6 spores (in 5 µL) of *S. ambofaciens* ATCC23877 were spotted on a sterile cellophane covering the medium in the Petri dish. Thirty hours later, cells were harvested using a sterile cone and deposited into a tube containing 5 mL of cold ethanol. Cells were then harvested by centrifugation for 15 min at 4,000 *g* at 4°C, and stored at -20°C.

RNA extraction, sequencing and analysis was performed as previously described (27). The reads were mapped in terms of "Gene" and pseudogene features according to *S. ambofaciens* ATCC23877 annotation (GCF_001267885.1_ASM126788v1_genomic.gff – released 2022-04-14) and modified to include our own manual curation of Samy prophage annotation. The reference condition used to run the SARTools DESeq2-based R pipeline (32) was 24 h-growth in MP5 medium. Data were analyzed with R software (33). Gene ontology analysis g:Profiler:g:GOSt software (https://biit.cs.ut.ee/gprofiler/gost, version e109_eg56_p17_1d3191d) was performed as previously described (23). The 'mclust' R package (34) was used to identify the gene populations of Samy prophage transcriptomes, via a Gaussian finite mixture model fitted by the expectation-maximization algorithm.

Virion purification by CsCl gradient

About 2.10^6 spores of *S. ambofaciens* ATCC 23877 were inoculated in 2 L of BM medium. After 4 days-growth, the culture was centrifuged at 8,000 rpm (JA14 rotor, Beckman) for 15 min at 4°C to pellet intact bacteria and debris. The supernatant was then transferred to new centrifuge tubes and subjected to overnight centrifugation under the same condition. The pellet was resuspended in 18 mL of TBT buffer and treated with 2 U/mL TURBO DNAse (Invitrogen) and 100 µg/mL RNAse for 1 h at 37°C. The phage was purified by isopycnic centrifugation in a CsCl discontinuous gradient for 5 h at 32,000 rpm in a SW41 rotor (Beckman) at 20°C, as previously described (35).

Transmission electron microscopy (TEM)

Phage samples collected after 4 days-growth in 1 L of HT liquid medium were concentrated for TEM observation by successive washes in ammonium acetate as previously described (36). To eliminate debris and/or dextrin, a second set of TEM observations using the negative staining method was conducted on CsCl-purified particles produced in BM medium. Three µl of sample suspension were deposited on an air glow-discharged 400 mesh copper carbon-coated grid for 1 min. Excess liquid was blotted, and the grid rinsed with 2 % w/v aqueous uranyl acetate. The grids were visualized at 100 kV with a Tecnai 12 Spirit TEM microscope (Thermo Fisher, New York NY, USA) equipped with a K2 Base 4k x 4k camera (Gatan, Pleasanton CA, USA).

Virome sequencing and data processing

DNA from CsCl-purified particles was extracted twice with phenol, once with chloroform, and dialyzed overnight against 10 mM Tris–HCl (pH 7.5) and 0.1 mM EDTA. After random fragmentation, the DNA sample was paired-end sequenced using Illumina dye sequencing as previously described (37). Data were analyzed with the Integrative Genomics Viewer (IGV) tool (38). STAR software (39) and *featureCounts* program (40) were used to quantify total reads along the reference genome containing only one terminal inverted repeat (TIR). The sequence coverage at termini position was identified using PhageTerm (Version 1.0.12) (41).

RESULTS

Identification of Samy, a complete prophage, in the *S. ambofaciens* ATCC 23877 chromosome

The comparison of *S. ambofaciens* ATCC 23877 genome to the closely related strain DSM 40697 led to the identification of a remarkably large genomic island (≈ 71 kb) in the terminal compartment (**Fig. 1A**). This region presents the lowest GC content (66.0 %) of the chromosome (**Fig. 1A**). PHASTER, a prophage prediction tool, detected in this genomic island a complete prophage, further named 'Samy'. A homology search determined that this prophage is specific to strain ATCC 23877. Its absence in the DSM 40697 strain indicates that the infection is relatively recent, *i.e.* occurred after speciation. The identification of a direct repeat ('TCGGGTGTGTCG') in front of a serine integrase gene and approximately 61 kb downstream prompted us to propose this sequence as belonging to the left (*attL*) and right (*attR*) attachment sites of the Samy prophage (6,589,778-6,650,857 bp position in the *S. ambofaciens* ATCC 23877 chromosome). Immediately upstream, a region of approximately 10 kb contains only a few phage genes, including one coding for a putative integrase, indicating that it may correspond to a remnant prophage (**Fig. 1B**). The mosaic composition of the genomic island suggests that it is located in a region prone to integration and/or fixation of exogenous sequences.

Samy prophage presents a typical GC content and size compared to other *Streptomyces phages* (**Fig. S1,** Supplementary **Table S4**). Annotation of Samy sequence allowed identification of most structural genes that are essential to form a caudate phage (*e.g.* encoding head, neck and tail proteins, base plate and tail fiber proteins) as well as replication proteins, endolysin, several nucleases, transcriptional regulators, integrase and recombination directionality factor (**Fig. 1.C**, Supplementary **Table S5**). Altogether, these analyses suggested that this prophage was complete and able to produce viral particles. This led us to investigate the conditions for its expression.

Activation of Samy prophage and other mobile genetic element expression is correlated with a general stress response

The terminal compartments of *Streptomyces* are less prone to transcription than the rest of the chromosome (23,27). Indeed, the expression of the highly variable regions enriched in those compartments is generally conditional. An empirical approach is often required to characterize the inducing conditions such as the OSMAC ("One Strain Many

Compounds") approach, based on strain cultivation in different environmental conditions (42). We used a similar approach by analyzing the Samy transcriptome in 13 growth conditions (**Fig. 2**, Supplementary **Fig. S2** and **Table S5**). We observed three conditions of 30 h growth on plates (named 'HT', 'ONA' or 'NAG') in which Samy prophage is globally expressed, suggesting that the lytic cycle of Samy was induced. The 'HT' condition had the strongest transcription level (**Fig. 2.A**). Interestingly, this condition is also associated with strong expression of several sequences from mobile genetic elements: the pSAM1 plasmid (**Fig. 2.B,** Supplementary **Fig. S3.A**), the integrative conjugative element (ICE) pSAM2 (**Fig. 1.A** & **2.B,** Supplementary **Fig. S3.B**) as well as several other genes of phage origin such as genes encoding a phage tail sheath protein (SAM23877_RS16255), two phage tail proteins (SAM23877_RS16260, SAM23877_RS23520) and a phage holin family protein (SAM23877_RS09270). We confirmed that Samy phage was produced in HT but not MP5 medium by performing PCR amplification of the region encompassing the 12-bp repeat with either divergent primers within the prophage (around the *attP* site) or convergent primers surrounding the prophage (around the *attB* site) (Supplementary **Table S2**).

We analyzed Samy transcriptomes in non or poorly inducing conditions (> 38 % of Samy genes remaining in the lowest 'CAT_0' category *i.e.* all conditions except 'HT', 'ONA', 'NAG'). In these conditions, the Samy transcriptome presents a bimodal pattern, as previously described for other phages (36) (Supplementary **Fig. S4**). The most transcribed genes in non or poorly inducing conditions could be involved in the lysogenic cycle of Samy or could be morons, *i.e.* genes involved in the fitness of the bacteria under these growth conditions or in their resistance to other phages (**Fig. 2.A,** Supplementary **Table S6**). Among them, the gene we annotated as a putative immunity repressor (SAMYPH_32/SAM23877_6125) was highly expressed under all conditions tested, reinforcing our prediction.

We determined host transcriptome characteristics during Samy awakening by comparing the three conditions associated with Samy induction ('HT', 'ONA', 'NAG') to the closest control condition, lacking Samy induction, identified by multidimensional analyses (Supplementary **Fig. S2.B & C**). This latter corresponds to 30 h growth on mannitol minimal medium plate ('MM' condition). GO enrichment and DESeq2 analyses revealed that Samy is induced in conditions associated with a strong repression of genes related to nitrogen assimilation (Supplementary **Table S5**). Several genes linked to adaptation to osmotic and oxidative stresses are also co-up-regulated with Samy. They notably encode gas vesicles, ectoine and ergothioneine biosynthesis processes (Supplementary **Table S5**). Moreover,

several sigma factors are differentially expressed in the ‘HT’ condition (compared to the ‘MM’ condition): six are induced including SigE, a regulator of cell envelope integrity (43) and SigF which is required for sporulation (44). Ten sigma factors are repressed including the principal sigma factor SigA (Supplementary **Table S5**). Altogether, these data indicate that the 'HT' condition is associated with a profound transcriptional change, probably reflecting a stressful situation.

In parallel, the genes in the GO functional categories ‘translation’ and ‘arginine biosynthetic process’ were strongly repressed (adjusted *p* values, calculated by g.Profiler, of $3.7x10^{-6}$ and $5.6\ x10^{-6}$, respectively). Indeed, 34 host tRNAs were repressed whereas all 4 of Samy’s tRNAs were induced. This illustrates how tRNA transduction can be part of phage expression strategy in a translation inhibiting situation.

The SOS response is classically associated with the activation of prophages, and has recently been described in *S. venezuelae* (45). In *S. ambofaciens* ATCC 23877, transcripts of the key actors of the SOS response such as RecA, LexA, RecN, DnaE, RuvA Holliday junction DNA helicase (45) were not up-regulated in the ‘HT’ condition compared to the ‘MM’ reference (Supplementary **Table S5**). This result suggests that the SOS response is not involved in the induction of Samy production in the ‘HT’ condition, or may be so transient and/or only present in part of the cell population that it was not detected by our bulk transcriptome analysis. Moreover, addition of mitomycin C DNA crosslinker and ciprofloxacin topoisomerase poison in MP5 medium, at the minimal concentrations that inhibit bacterial growth (1 and 2 µg/mL, respectively), did not induce Samy production (negative results, not shown). This observation reinforces the hypothesis that the SOS response may not be involved in the induction of Samy under our study conditions.

To conclude, in our study the activation of Samy and other genetic elements is correlated with huge physiological changes associated notably with nitrogen imbalance and translation inhibition and a general stress response.

Samy production increases in alkaline conditions

In order to determine the key compounds responsible for Samy induction, and to set up monitoring of its production in liquid medium, we tested variants of the HT liquid medium by eliminating one or more of its constituents. The simplest version of a medium associated with high viral titers, as quantified by qPCR, was named "BM" (for “Bacteriophage production Medium”) (**Fig. 3**). We noted a fairly high inter-experimental variability in Samy titer in BM medium, which might reflect its stochasticity within the cell population. However,

production kinetics is the same in all experiments: Samy particles are released between 24 and 48h of growth in BM medium, the titer being almost constant over the following days (**Fig. 4.A**).

Interestingly, we observed increased phage production in the absence of buffering compounds such as dextrin or MOPS (**Fig. 3**). The correlation between viral titer and pH is statistically significant (Spearman's rank correlation rho = 0.73, *p* value = 0.016), indicating that alkalinity constitutes an additional signal triggering Samy production and/or increasing virion stability in the supernatant.

Samy is a new active siphovirus

TEM revealed that Samy is a siphovirus with a capsid diameter of 65.4 ± 2.8 nm (*n* = 35), and a long rather rigid tail 248.7 ± 7.4 nm in length (*n* = 32) and 11.7 ± 0.4 nm thick (*n*=12) (**Fig. 4B**, Supplementary **Fig. S5.A-C**). Remarkably, Samy virions are co-purified with phage tail-like nanostructures (Supplementary **Fig. S5.A**), previously identified as extracellular contractile injection systems (46,47). Consistently, the transcription of the orthologous genes encoding this system in *S. ambofaciens* ATCC 23877 (SAM23877_RS16255, SAM23877_RS16260) is induced in the 'HT' condition (Supplementary **Table S5**).

High-throughput sequencing of these CsCl-purified particles revealed that Samy phage is the only double stranded DNA phage produced in this condition. In total, 8,671,900 (99.5%) out of 8,712,953 reads successfully aligned to the *S. ambofaciens* ATCC 23877 genome corresponded to Samy. The remaining reads mapped all along the *S. ambofaciens* genome and may correspond to contaminating bacterial DNA and/or transduced DNA. Reads confirmed the borders of the prophage and did not show any trace of lateral transduction, consistent with a *cos* packaging mechanism (Supplementary **Fig. S6**).

Finally, Samy virions are infectious since we observed plaques using *Streptomyces lividans* TK24 strain as a host (Supplementary **Fig. S5.D**). Strikingly, no lysis plaque could be obtained during the infection assays conducted on 7 other strains listed in Supplementary **Table S1**, including two S. *ambofaciens* strains. The absence of superinfection of strain ATCC 23877 is expected, since prophage-bearing strains generally express an immunity repressor. For the other strains, these results indicate that Samy

infection has a fairly narrow spectrum and/or requires lab conditions that were not reproduced in these experiments.

Altogether, these results indicate that Samy is an active prophage that encodes a complete and infectious siphovirus.

Impact of Samy phage on *Streptomyces* growth

We first compared ATCC 23877 (Samy$^+$) and DSM 40697 (Samy$^-$) strain growth in BM medium, using MP5 medium as a control. Surprisingly, the exponential phase of growth started about 8 h earlier in BM than in MP5 medium, suggesting that germination was more efficient or rapid in this condition (**Fig. 5.A**). At later stages of growth, the increase in biomass stopped in BM medium quite early (at a pseudo-opacimetry of about 1) whereas it reached higher densities in MP5 medium (**Fig. 5.A**). We found that this cessation of growth in BM medium correlated with the alkalinity of the medium (**Fig. 5.A**). In addition, both strains presented different phenotypes in the following days of growth in BM medium: while the strain ATCC 23877 remained relatively dispersed at a density that did not drop much, strain DSM 40697 formed large pellets (**Fig. 5.B**).

We used a CRIPSR approach to obtain ATCC 23877 derivates deleted for part or all of the prophage (Supplementary **Table S1**). Although the three clones tested carry different Samy deletions, they all presented the same phenotype. After 4 days of growth, aggregates appeared in the cultures, but not in the parental strain (**Fig. 5.B**). Microscopic observations of the cultures confirmed the formation of larger and denser cell pellets in the absence of the prophage (**Fig. 5.C,** Supplementary **Fig. S7.A**). Furthermore, analysis of the growth of another *Streptomyces* species, *S. coelicolor* A(3)2, reinforces the observation that the formation of cell aggregates is a rather standard phenotype in BM medium of *Streptomyces* species that do not contain Samy prophage (Supplementary **Fig. S7.B**).

Because of the multicellular nature of *Streptomyces*, the CFU count not only reflects cell survival, but also the number of multicellular clusters *per se* regardless of the number and proportion of living or dying cells in the clusters. Thus, we hypothesized that Samy induction could modify the number of culturable and viable colonies in the medium. We then determined the number of CFUs on SFM medium after 4 days in the strains ATCC 23877 (Samy$^+$), DSM 40697 (Samy$^-$) and ATCC 23877 Δ*Samy*. Remarkably, this number was around 2-logs higher in the phage-producing ATCC 23877 strain than in its phage-deleted derivative or the DSM 40697 strain (**Fig. 5.D**). Thus, the activation of Samy prophage was correlated with a drastic increase in the number of viable multicellular clusters formed by

the ATCC 23877 parental strain. During a return to a condition more favorable to growth (exemplified here by the SFM medium used to count the colonies), this property resulted in an increase in the number of CFUs compared to strains having formed larger cell aggregates.

To evaluate the potential impact of storage and strain evolution in laboratory conditions on the growth phenotype, we performed a comprehensive analysis on multiple *S. ambofaciens* strains (harboring or not Samy prophage) sourced from diverse collections (Supplementary **Table S1**). Once again, we observed a positive correlation (R = 0.75, p = 0.00074, Spearman method) between the production of Samy and the number of CFUs following a four-day growth period in BM medium (**Fig. 5.E**).

In order to test whether a soluble factor present in the culture supernatant could contribute to the dispersal phenotype, we added a conditioned supernatant of the parental strain grown 4 days in BM medium to a 24 h culture of the phage-deleted strain. We found no increase in colony number after 4 days of incubation in BM medium (Supplementary **Fig. S8**), indicating that the prophage needs to be present within the cells to increase the dispersal.

Altogether these results indicate that the expression and production of Samy prevents the formation of large cell aggregates by *S. ambofaciens* ATCC 23877 in a stressful condition, promoting bacterial dispersal (and possibly survival) at the population level.

Impact of Samy phage on antibacterial activity

Finally, we evaluated the impact of Samy phage production on antibacterial activity, a key step in the development cycle of *Streptomyces*. Interestingly, the antibacterial activity of the ATCC 23877 strain in BM condition is not affected by the presence or absence of an intact prophage copy (**Fig. 5.F**). This suggests that the production of phages is not associated with massive death of antibiotic-producing cells.

DISCUSSION

In this study we describe the conditions of awakening of a *Streptomyces* prophage associated with profound physiological changes within the colony. Initially, the HT medium was developed by Hickey and Tresner (48) to induce sporulation of *Streptomyces* strains that sporulate poorly on growth media classically used for this purpose. In the same condition, using transcriptomics analyses, we have described for the first time a massive

activation of mobile genetic element expression (Samy prophage, pSAM1 plasmid and pSAM2 ICE; **Fig. 2,** Supplementary **Fig. S3**) as well as other phage-related genes such as those encoding phage tail-like nanostructures (46,47) (Supplementary **Fig. S5.A** and **Table S5**).

This phenomenon seems to be concomitant with physiological modifications that may contribute to strain dispersal in stress conditions. For instance, we observed increased expression of the genes encoding the synthesis of geosmin and 2-methylisoborneol volatile compounds (Supplementary **Table S5**) which may promote spore dispersal by animals (8,49). Moreover, a hydrophobic layer of chaplins may also contribute to their dispersion by limiting their loss in the anoxic depths of the soil, and by mediating their adhesion to hydrophobic surfaces (50). The induction of the expression of genes encoding gaseous vesicles (Supplementary **Table S5**) may also contribute to the flotation and propagation of *Streptomyces* (51). Phage production thus seems to be part of a dispersal strategy.

The precise signal for Samy prophage induction has yet to be determined. The transcriptome analysis after 30 h growth on HT solid medium reflects a high stress situation associated with an imbalance in nitrogen metabolism and translation inhibition (Supplementary **Table S5**). Alkalinity constitutes an additional stress signal stimulating Samy exit from dormancy or enhancing phage particle stability (**Fig. 3**). Interestingly, alkaline conditions are also required for the initiation of the ‘explorer’ phenotype in *S. venezuelae* (52).

Most of our experiments were conducted under liquid growth conditions, a situation actually similar to those of most industrial bioreactors. It has long been described that the appearance of *Streptomyces* growth in liquid media (dispersed hyphae *versus* pellets or clumps) depends on the state of the initial inoculum and varies from one species to another (53). “Fragmentation of the mycelial clumps” (54) or “pellet fragmentation” (55) in liquid medium have even been reported for some species. The biophysical parameters that may influence the type of hyphae grouping in liquid medium have been explored for a few strains (42). Some genetic factors such *ssgA* morphogene (54) also contribute to the morphology of *Streptomyces* mycelia in submerged cultures. Mycelium fragmentation may actually be a key contributor to strain spread in liquid medium, since most *Streptomyces,* like *S. ambofaciens* ATCC 23877, sporulate poorly or not at all during submerged growth. In this study, we demonstrate for the first time that a prophage can contribute to a similar process by promoting the formation of small and numerous clumps favoring strain dispersal, and increasing by 2-logs the number of clumps/pellets able to give rise to new colonies. Samy

belongs to the group of Caudovirales which are released by cell lysis. So we propose that cell death induced by Samy in part of the colony contributes to this strain dispersal (**Fig. 6**). The fact that partial deletion of Samy (in the integrase coding region) is sufficient to abolish the phenotype, supports the view that viral production is required.

Samy phage production takes place mainly between 24 h and 48 h of growth in BM medium (**Fig. 4.A**), leading to a final phage titer that is quite variable from one experiment to another (**Fig. 3**). This suggests that the triggering of phage production in the population may be stochastic. Only a portion of the cells die as evidenced by the lack of impact on overall antibiotic production in BM liquid medium (**Fig. 5.F**), the high number of CFU after 4 days-growth in this medium (**Fig. 5.D**) and the effective sporulation of the strain on solid HT medium (our personal observations). The fact that the putative immune repressor is still expressed in 'HT' conditions reinforces these observations as this is characteristic of transcriptomes made on heterogeneous populations with respect to phage production, as previously reported (36). Thus, we favor a model in which only a fraction of the cells will die, allowing the preservation of the remainder of the colony or cell aggregate. Altogether, Samy production may be considered an additional example of division of labor which can lead to the 'altruistic' loss of fitness of a subpopulation of the cells (57).

The similarities between *Streptomyces* mycelium fragmentation and biofilm dispersal have been previously highlighted (55). Moreover, the use of phages is presented as a promising approach to control biofilms (58). Our study highlights the possible risk of bacterial dispersal that may be associated with the (partial) production of phages in cellular aggregates. Phage-mediated dispersal of biofilms has also been reported in *Enterococcus faecalis* unicellular bacteria (25). Another prophage, in *Pseudomonas aeruginosa*, has already been shown to have an impact on bacterial biofilms by consolidating them through the contribution of extracellular DNA (59). Our study further emphasizes the importance of considering prophages in biofilm/aggregate dynamics since they can provide positive fitness at the strain/cell population level.

In conclusion, this study sheds new light on the role of phages in soil ecology via dispersion of multicellular colonies, and illustrates the potential role of phage-imposed selection for evolved trade-ups in host bacteria (60). The system may also be of interest for theoretical considerations of the role of dispersion in transitions to multicellular life (61).

Data Availability

The RNA-seq data generated during this study have been deposited in the NCBI Gene Expression Omnibus (GEO, https://www.ncbi.nlm.nih.gov/geo/) under the accession code **GSE232795** (https://www-ncbi-nlm-nih-gov.insb.bib.cnrs.fr/geo/query/acc.cgi?acc=GSE232795). The virome sequencing data are avalaible in the bioproject PRJNA974565 on **SRA** (https://www.ncbi.nlm.nih.gov/bioproject/974565). We used RNA-seq data available under the accession code **GSE162865** (https://www-ncbi-nlm-nih-gov.insb.bib.cnrs.fr/geo/query/acc.cgi?acc=GSE162865) (27).

APPENDICES

Supplementary Fig. S1: GC content (A) and size (B) of a panel of 330 *Streptomyces* phages

Supplementary Fig. S2: Multidimensional analyses of the transcriptomes of *S. ambofaciens* ATCC 23877 grown under various conditions

Supplementary Fig. S3: Heatmaps of pSAM1 (A) and pSAM2 (B) transcriptomes in different growth conditions

Supplementary Fig. S4: Samy expression profile under the different conditions studied

Supplementary Fig. S5: Samy phage morphology and infection assays

Supplementary Fig. S6: Results of high-throughput sequencing of the double-stranded DNA virome of *Streptomyces ambofaciens* ATCC 23877 grown 4 days in BM medium

Supplementary Fig. S7: Morphology of *S. ambofaciens* and *S. coelicolor* after 4 days growth in BM medium

Supplementary Fig. S8: Counting colony-forming units after 4 days of growth in BM medium of *S. ambofaciens* ATCC 23877 reference strain and its isogenic ΔSamy #clone 3 mutant supplemented with conditioned supernatants

Supplementary Table S1: Strains used in this study

Supplementary Table S2: Primers used in this study

Supplementary Table S3: Media used in this study

Supplementary Table S4: List and characteristics of 330 *Streptomyces* phages referenced in Actinophage Database, NCBI and/or ICTV. The legend is detailed in the “Readme” sheet.

Supplementary Table S5: Results from the OSMAC-RNAseq approach conducted in *Streptomyces ambofaciens* ATCC 23877. The legend is detailed in the “Readme” sheet.

Supplementary Table S6: List of Samy genes overexpressed in non or poorly inducing conditions. The legend is detailed in the “Readme” sheet.

ACKNOWLEDGMENTS

This work was supported by the *Agence Nationale pour la Recherche* [ANR-21-CE12-0044-01/STREPTOMICS]. We thank Jean-Luc Pernodet and Frederic Boccard for their precious support. We also would like to thank Christine Longin (MIMA2 platform) for her help with TEM observations and Julien Lossouarn for his help in annotating phage genes and submitting Samy's genome. We thank Soumaya Najah and Corinne Saulnier for their technical help. We are grateful to Vinciane Regnier and Logan Greibill for valuable training on the Olympus BX63 microscope. We also thank Pascaline Tirand for her daily help.

CONFLICT OF INTEREST

The authors declare no competing interests.

REFERENCES

1. Berdy J. Thoughts and facts about antibiotics: where we are now and where we are heading. J Antibiot (Tokyo). 2012;65(8):385-95.
2. Donald L, Pipite A, Subramani R, Owen J, Keyzers RA, Taufa T. *Streptomyces*: Still the Biggest Producer of New Natural Secondary Metabolites, a Current Perspective. Microbiology Research. 1 2022;13(3):418-65.
3. Barka EA, Vatsa P, Sanchez L, Gaveau-Vaillant N, Jacquard C, Meier-Kolthoff JP, et al. Taxonomy, Physiology, and Natural Products of Actinobacteria. Microbiol Mol Biol Rev. 2016;80(1):1-43.
4. Prudence SMM, Addington E, Castaño-Espriu L, Mark DR, Pintor-Escobar L, Russell AH, et al. Advances in actinomycete research: an ActinoBase review of 2019. Microbiology. 2020;166(8):683-94.
5. Jones SE, Elliot MA. *Streptomyces* Exploration: Competition, Volatile Communication and New Bacterial Behaviours. Trends in Microbiology. 2017;25(7):522-31.
6. Russell DA, Hatfull GF. PhagesDB: the actinobacteriophage database. Wren J, Bioinformatics. 2017;33(5):784-6.
7. Krishnamurthy SR, Janowski AB, Zhao G, Barouch D, Wang D. Hyperexpansion of RNA Bacteriophage Diversity. PLoS Biol. 2016;14(3):e1002409.
8. Shepherdson EM, Baglio CR, Elliot MA. *Streptomyces* behavior and competition in the natural environment. Current Opinion in Microbiology. 2023;71:102257.
9. Lu N, Kim C, Chen Z, Wen Y, Wei Q, Qiu Y, et al. Characterization and genome analysis of the temperate bacteriophage φSAJS1 from *Streptomyces avermitilis*. Virus Research. 2019;265:34-42.
10. Hardy A, Sharma V, Kever L, Frunzke J. Genome Sequence and Characterization of Five Bacteriophages Infecting *Streptomyces coelicolor* and *Streptomyces venezuelae*: Alderaan, Coruscant, Dagobah, Endor1 and Endor2. Viruses. 2020;12(10):1065.
11. Luthe T, Kever L, Hänsch S, Hardy A, Tschowri N, Weidtkamp-Peters S, et al. *Streptomyces* development is involved in the efficient containment of viral infections. microLife. 2023;4:uqad002.
12. Kronheim S, Daniel-Ivad M, Duan Z, Hwang S, Wong AI, Mantel I, et al. A chemical defence against phage infection. Nature. 2018;564(7735):283-6.
13. Kever L, Hardy A, Luthe T, Hünnefeld M, Gätgens C, Milke L, et al. Aminoglycoside Antibiotics Inhibit Phage Infection by Blocking an Early Step of the Infection Cycle. mBio. 2022;13(3):e00783-22.
14. Hardy A, Kever L, Frunzke J. Antiphage small molecules produced by bacteria – beyond protein-mediated defenses. Trends in Microbiology. 2023;31(1):92-106.
15. Sharma V, Hardy A, Luthe T, Frunzke J. Phylogenetic Distribution of WhiB- and Lsr2-Type Regulators in Actinobacteriophage Genomes. Microbiol Spectr. 2021;9(3):e00727-21.
16. Rosner A, Gutstein R. Adsorption of actinophage Pal 6 to developing mycelium of *Streptomyces albus*. Can J Microbiol. 1981;27(2):254-7.
17. Jordan TC, Burnett SH, Carson S, Caruso SM, Clase K, DeJong RJ, et al. A Broadly Implementable Research Course in Phage Discovery and Genomics for First-Year Undergraduate Students. mBio. 2014;5(1):e01051-13.
18. Fogg PCM, Haley JA, Stark WM, Smith MCM. Genome Integration and Excision by a New *Streptomyces* Bacteriophage, ϕJoe. Appl Environ Microbiol. 2017;83(5):e02767-16.
19. Sharaf A, Mercati F, Elmaghraby I, Elbaz RM, Marei EM. Functional and comparative genome analysis of novel virulent actinophages belonging to *Streptomyces flavovirens*. BMC Microbiol. 2017;17(1):51.

20. Ongenae V, Azeredo J, Kropinski AM, Rozen D, Briegel A, Claessen D. Genome sequence and characterization of *Streptomyces* phage Pablito, representing a new species within the genus Janusvirus. Sci Rep. 2022;12(1):17785.

21. Park YG, McCarthy GF, Mustafa H, Feild GM, Puram S, Younes HA, et al. Complete Genome Sequences of *Streptomyces* Bacteriophages Annihilus, TonyStarch, Thiqqums, CricKo, ClubPenguin, RosaAsantewaa, and PherryCruz. Microbiol Resour Announc. 2022;11(11):e00922-22.

22. Arndt D, Grant JR, Marcu A, Sajed T, Pon A, Liang Y, et al. PHASTER: a better, faster version of the PHAST phage search tool. Nucleic Acids Res. 2016;44(W1):W16-21.

23. Lorenzi JN, Thibessard A, Lioy VS, Boccard F, Leblond P, Pernodet JL, et al. Ribosomal RNA operons define a central functional compartment in the *Streptomyces* chromosome. Nucleic Acids Research. 2022;50(20):11654-69.

24. Taylor VL, Fitzpatrick AD, Islam Z, Maxwell KL. The Diverse Impacts of Phage Morons on Bacterial Fitness and Virulence. In: Advances in Virus Research. Elsevier; 2019. p. 1-31. https://linkinghub.elsevier.com/retrieve/pii/S0065352718300435

25. Rossmann FS, Racek T, Wobser D, Puchalka J, Rabener EM, Reiger M, et al. Phage-mediated Dispersal of Biofilm and Distribution of Bacterial Virulence Genes Is Induced by Quorum Sensing. PLoS Pathog. 2015;11(2):e1004653.

26. Tong Y, Charusanti P, Zhang L, Weber T, Lee SY. CRISPR-Cas9 Based Engineering of Actinomycetal Genomes. ACS Synth Biol. 2015;4(9):1020-9.

27. Lioy VS, Lorenzi JN, Najah S, Poinsignon T, Leh H, Saulnier C, et al. Dynamics of the compartmentalized *Streptomyces* chromosome during metabolic differentiation. Nat Commun. 2021;12(1):5221.

28. Haas D, Barba M, Vincente C, Nezbedova S, Garénaux A, Hôtel L, et al. Synteruptor, a new comparative genomics-based approach for identifying non-classical specialized metabolite gene clusters. In preparation.

29. Thibessard A, Haas D, Gerbaud C, Aigle B, Lautru S, Pernodet JL, et al. Complete genome sequence of *Streptomyces ambofaciens* ATCC 23877, the spiramycin producer. J Biotechnol. 2015;214:117-8.

30. Zimmermann L, Stephens A, Nam SZ, Rau D, Kübler J, Lozajic M, et al. A Completely Reimplemented MPI Bioinformatics Toolkit with a New HHpred Server at its Core. Journal of Molecular Biology. 2018;430(15):2237-43.

31. Terzian P, Olo Ndela E, Galiez C, Lossouarn J, Pérez Bucio RE, Mom R, et al. PHROG: families of prokaryotic virus proteins clustered using remote homology. NAR Genomics and Bioinformatics. 2021;3(3):lqab067.

32. Varet H, Brillet-Gueguen L, Coppee JY, Dillies MA. SARTools: A DESeq2- and EdgeR-Based R Pipeline for Comprehensive Differential Analysis of RNA-Seq Data. PLoS One. 2016;11(6):e0157022.

33. R Core Team. R: A language and environment for statistical computing. R Foundation for Statistical Computing. 2022; URL https://www.R-project.org/

34. Scrucca L, Fop M, Murphy T Brendan, Raftery A E. mclust 5: Clustering, Classification and Density Estimation Using Gaussian Finite Mixture Models. The R Journal. 2016;8(1):289.

35. Jakutytė L, Baptista C, São-José C, Daugelavičius R, Carballido-López R, Tavares P. Bacteriophage Infection in Rod-Shaped Gram-Positive Bacteria: Evidence for a Preferential Polar Route for Phage SPP1 Entry in *Bacillus subtilis*. J Bacteriol. 2011;193(18):4893-903.

36. Misson P, Bruder E, Cornuault JK, De Paepe M, Nicolas P, Demarre G, et al. Phage production is blocked in the adherent-invasive *Escherichia coli* LF82 upon macrophage infection. PLoS Pathog. 2023;19(2):e1011127.

37. Djacem K, Tavares P, Oliveira L. Bacteriophage SPP1 pac Cleavage: A Precise Cut without Sequence Specificity Requirement. Journal of Molecular Biology. 2017;429(9):1381-95.

38. Robinson JT, Thorvaldsdottir H, Winckler W, Guttman M, Lander ES, Getz G, et al. Integrative genomics viewer. Nat Biotechnol. 2011;29(1):24-6.

39. Dobin A, Davis CA, Schlesinger F, Drenkow J, Zaleski C, Jha S, et al. STAR: ultrafast universal RNA-seq aligner. Bioinformatics. 2013;29(1):15-21.

40. Liao Y, Smyth GK, Shi W. featureCounts: an efficient general purpose program for assigning sequence reads to genomic features. Bioinformatics. 2014;30(7):923-30.

41. Garneau JR, Depardieu F, Fortier LC, Bikard D, Monot M. PhageTerm: a tool for fast and accurate determination of phage termini and packaging mechanism using next-generation sequencing data. Sci Rep. 2017;7(1):8292.

42. Bode HB, Bethe B, Hofs R, Zeeck A. Big effects from small changes: possible ways to explore nature's chemical diversity. Chembiochem. 2002;3(7):619-27.

43. Tran NT, Huang X, Hong H, Bush MJ, Chandra G, Pinto D, et al. Defining the regulon of genes controlled by σ^{E}, a key regulator of the cell envelope stress response in *Streptomyces coelicolor*. Mol Microbiol. 2019;112(2):461-81.

44. Tzanis A, Dalton KA, Hesketh A, Hengst CD, Buttner MJ, Thibessard A, et al. A sporulation-specific, *sigF* -dependent protein, SspA , affects septum positioning in *Streptomyces coelicolor* . Molecular Microbiology. 2014;91(2):363-80.

45. Stratton KJ, Bush MJ, Chandra G, Stevenson CEM, Findlay KC, Schlimpert S. Genome-Wide Identification of the LexA-Mediated DNA Damage Response in *Streptomyces venezuelae*. J Bacteriol. 2022;204(8):e00108-22.

46. Nagakubo T, Yamamoto T, Asamizu S, Toyofuku M, Nomura N, Onaka H. Phage tail-like nanostructures affect microbial interactions between *Streptomyces* and fungi. Sci Rep. 2021;11(1):20116.

47. Vladimirov M, Zhang RX, Mak S, Nodwell JR, Davidson AR. A contractile injection system is required for developmentally regulated cell death in *Streptomyces coelicolor.* Nat Commun. 2023;14(1):1469.

48. Hickey RJ, Tresner HD. A cobalt-containing medium for sporulation of *Streptomyces* species. J Bacteriol. 1952;64(6):891-2.

49. Becher PG, Verschut V, Bibb MJ, Bush MJ, Molnár BP, Barane E, et al. Developmentally regulated volatiles geosmin and 2-methylisoborneol attract a soil arthropod to *Streptomyces* bacteria promoting spore dispersal. Nat Microbiol. 2020;5(6):821-9.

50. Hopwood DA. *Streptomyces* in nature and medicine: the antibiotic makers. Oxford ; New York: Oxford University Press; 2007. 250 p.

51. Huang R, Lin J, Gao D, Zhang F, Yi L, Huang Y, et al. Discovery of gas vesicles in *Streptomyces sp.* CB03234-S and potential effects of gas vesicle gene overexpression on morphological and metabolic changes in *streptomycetes*. Appl Microbiol Biotechnol. 2019;103(14):5751-61.

52. Jones SE, Ho L, Rees CA, Hill JE, Nodwell JR, Elliot MA. *Streptomyces* exploration is triggered by fungal interactions and volatile signals. eLife. 2017;6:e21738.

53. Kieser T. BMJ Buttner MJ, Chater KF, Hopwood DA. Practical *Streptomyces* genetics. John Innes Foundation, Norwich, United Kingdom. 2000.

54. van Wezel GP, Krabben P, Traag BA, Keijser BJF, Kerste R, Vijgenboom E, et al. Unlocking *Streptomyces* spp. for Use as Sustainable Industrial Production Platforms by Morphological Engineering. Appl Environ Microbiol. 2006;72(8):5283-8.

55. Zacchetti B, Smits P, Claessen D. Dynamics of Pellet Fragmentation and Aggregation in Liquid-Grown Cultures of *Streptomyces lividans.* Front Microbiol. 2018;9:943.

56. Manteca A, Rioseras B, González-Quiñónez N, Fernández-García G, Yagüe P. Mycelium Differentiation and Development of *Streptomyces* in Liquid Nonsporulating Cultures: Programmed Cell Death, Differentiation, and Lysis Condition Secondary Metabolite Production. In: Growing and Handling of Bacterial Cultures. IntechOpen; 2019. https://www.intechopen.com/books/growing-and-handling-of-bacterial-cultures/mycelium-differentiation-and-development-of-em-streptomyces-em-in-liquid-nonsporulating-cultures-pro

57. Zhang Z, Shitut S, Claushuis B, Claessen D, Rozen DE. Mutational meltdown of putative microbial altruists in *Streptomyces coelicolor* colonies. Nat Commun. 2022;13(1):2266.

58. Chang C, Yu X, Guo W, Guo C, Guo X, Li Q, et al. Bacteriophage-Mediated Control of Biofilm: A Promising New Dawn for the Future. Front Microbiol. 2022;13:825828.

59. Rice SA, Tan CH, Mikkelsen PJ, Kung V, Woo J, Tay M, et al. The biofilm life cycle and virulence of *Pseudomonas aeruginosa* are dependent on a filamentous prophage. ISME J. 2009;3(3):271-82.

60. Burmeister AR, Turner PE. Trading-off and trading-up in the world of bacteria–phage evolution. Current Biology. 2020;30(19):R1120-4.

61. Black AJ, Bourrat P, Rainey PB. Ecological scaffolding and the evolution of individuality. Nat Ecol Evol. 2020;4(3):426-36.

62. Smith MCM, Burns RN, Wilson SE, Gregory MA. The complete genome sequence of the *Streptomyces* temperate phage C31: evolutionary relationships to other viruses. Nucleic Acids Research. 1999;27(10):2145-55.

63. Khaleel T, Younger E, McEwan AR, Varghese AS, Smith MCM. A phage protein that binds φC31 integrase to switch its directionality: Excision by φC31 integrase. Molecular Microbiology. 2011;80(6):1450-63.

Figure Legends

Figure 1: Samy prophage identification by comparative genomics

A. Pairwise comparison of *S. ambofaciens* ATCC 23877 and DSM 40697 chromosomes. The grey line indicates the position of genes whose order is perfectly conserved between strains. The blue dots indicate areas of synteny break. The red circles correspond to genomic islands containing at least 20 CDS in one of the strains. The blue arrows indicate the position of xSAM1-pSAM2 integrated elements as well as the genomic island of interest harboring Samy prophage, detailed in the panels B and C. The central compartment (delimitated by the distal *rrn* operons) (27), the arms (defined as terminal regions devoid of core genes), the terminal inverted repeats (TIRs) and the position of the origin of replication (*oriC*) in *S. ambofaciens* ATCC 23877 chromosome are indicated. The level of gene order conservation between both strains as well as the GC percent content calculated in a window of 50 kb are indicated below the dot-blot.

B. Schematic representation of the genomic island containing the Samy prophage. The regions in which gene order is perfectly conserved in *S. ambofaciens* ATCC 23877 and DSM 40697 chromosomes are defined as the left and right synteny blocks (grey). The coordinates of the genomic island borders in *S. ambofaciens* ATCC 23877 strain are indicated in blue. The genomic island is composed of two regions: a remnant integrative element and the Samy prophage. These regions are separated by a short intergenic region (represented by an asterisk; 305 bp located from 6,589,473 to 6,589,777 bp) present in both strains. Two serine integrase coding sequences (red) have been predicted. The prophage also contains four tRNA encoding genes (pink).

C. Comparison of the Samy and PhiC31 phage genomes. Gene functions are color-coded as detailed in the legend. The annotation of PhiC31 genes was previously reported in (62) and (63) (for the recombination directionality factor, RDF). Black vertical lines indicate the nine Samy genes identified as overexpressed compared to the entire Samy phage genome across all non or poorly-induced conditions (Supplementary **Table S6**). The genome comparison was performed using Easyfig software (e-value $<10^{-3}$). The percentage identity between DNA homologous sequences in Samy and PhiC31 is shown in shades of gray. Other abbreviations: DNK (Deoxynucleoside monophosphate kinase), MCP (major capsid protein), MTP (Major tail protein), TSS (Terminal small subunit), TLS (Terminal large subunit), TMP (Tape measure protein).

Figure 2: Massive awakening of mobile genetic elements in HT medium

A. Heatmap of Samy region transcription in different growth conditions. Normalized RNA-seq data (Supplementary **Table S5**) were categorized in a color scale reflecting the expression of each gene relative to whole genome expression in each condition, as indicated in the Annotation legend. Each line represents a gene, ranked according to their order on the genome. For the remnant integrative element as well as for Samy prophage, a prediction of the gene product is indicated when available. Growth conditions (columns) are ranked by hierarchical clustering according to Samy transcriptome profiles. The growth conditions are detailed in Supplementary **Fig. S2.A** and **Table S3**. Phage genes of predicted function that stand out as overexpressed compared to the entire Samy phage genome across at least six non or poorly-induced conditions (Supplementary **Table S6**) are written in bold.

B. Plot of the log ratio of differential expression as a function of gene expression after 30 h growth in HT solid medium compared to 24 h growth in liquid MP5 medium.

The color of differentially expressed genes (adjusted *p* value < 0.05) is indicated. The number of regulated genes relative to the total number of genes is shown in parentheses for the mobile genetic elements of interest.

Figure 3: Impact of medium composition on Samy phage production, final pH and antibacterial activity of *S. ambofaciens* ATCC 23877 supernatants

The supernatants of *S. ambofaciens* ATCC 23877 grown in different media (Supplementary **Table S3**) were harvested after 4 days and 0.2 µm-filtered. Phage titer was determined by qPCR after DNAse treatment. The pH of the medium and the antibacterial activity against *Micrococcus luteus* of the supernatant after 4 days of growth are indicated on the top. All media had an initial pH of 7.3 (± 0.1), except MP5 and MP5 devoid of MOPS which had a pH of 7.5 (± 0.1). All the boxplots represent the first quartile, median and third quartile. The upper whisker extends from the hinge to the largest value no further than 1.5 * the inter-quartile range (IQR, *i.e*. distance between the first and third quartiles). The lower whisker extends from the hinge to the smallest value at most 1.5 * IQR of the hinge. Each dot represents an independent experiment. The *p* values of two-sided Wilcoxon rank sum tests with continuity correction is indicated for each comparison to the viral titer observed in HT condition.

Figure 4: Samy phage production and morphology

A. Kinetics of phage production. *S. ambofaciens* ATCC 23877 was grown in BM medium. The viral titer of supernatants filtered and DNAse-treated were determined by qPCR. Each color represents an independent experiment. The boxplot is plotted as described in the legend to **Fig. 3**. The *p* value of two-sided Wilcoxon rank sum tests with continuity correction is 0.0294 when comparing the viral titers at 24 h and 48h, and 1 (no difference) when comparing the evolution of the titer on the following days.

B. Imaging of Samy phage produced by transmission electron microscopy. *S. ambofaciens* ATCC 23877 was grown during 4 days in BM medium. The supernatant was concentrated by CsCl-gradient ultracentrifugation. Viral particles were negatively stained with uranyl acetate. Scale bar: 100 nm.

Figure 5: Dispersion phenotype associated with the production of the Samy phage

A. Growth and pH in BM and MP5 media. Each symbol represents an independent experiment. Due to the presence of large aggregates (see panel B), the pseudo-opacimetry ($OD_{600\ nm}$) was not exploitable for DSM 40697 strain after 48h of growth in BM medium.

B. Dispersed *versus* aggregated growth of *S. ambofaciens* strains in BM media. The results are representative of the appearance of the most frequently observed cultures, as the quantity and size of cell clusters may vary from one experiment to the other. The *S. ambofaciens* ATCC 23877 Δ*Samy* strain corresponds to clone #3, deleted from at least the phage integrase by a CRIPSR-based approach (Supplementary **Table S1**). Scale bar: 1.5 cm.

C. Microscopy of *Streptomyces* colonies after 4 days growth in BM medium. *S. ambofaciens* ATCC 23877 and its derivate CRISPR-deleted of Samy prophage (clone #3) were grown in BM medium and imaged using differential interference contrast microscopy (also see Supplementary **Figure S7.A**). Scale bar: 10 µm.

D. Colony forming units after 4 days of growth in BM medium. The *S. ambofaciens* ATCC 23877 ΔSamy strains correspond to three independent mutants (#1, #3 and #4) we obtained by a CRIPSR-based approach (Supplementary **Table S1**). The boxplot is plotted as described in the legend to **Fig. 3**. Each dot represents an independent experiment per condition. The *p* values of two-sided Wilcoxon rank sum tests with continuity correction are indicated for each comparison. Please note that this number is the result of both cell survival and mycelium dispersal (propensity to form separate colonies).

E. Correlation between Samy phage production and colony forming units by diverse *S. ambofaciens* strains. *S. ambofaciens* strains obtained from distinct collections (Supplementary **Table S1**) were grown during 4 days in BM medium, before counting colony forming units and phage production in the supernatants. Even strains ATCC 23877 and DSM 40697 were cultured for this experiment from stocks produced by another laboratory. Each dot represents an independent experiment per strain. The correlation was analyzed by a Spearman's rank correlation test. Results of two independent experiments.

F. Bioassay performed with the supernatants of *S. ambofaciens* ATCC 23877 WT strain and its derivatives deleted in Samy regions (clones #1, #3 and #4 - Supplementary **Table S1**) cultures grown during 4 days in BM medium. The boxplot is plotted as described in the legend of **Fig. 3**. The *p* values of two-sided Wilcoxon rank sum tests with continuity correction are indicated.

Figure 6: Model of the stress- and phage-induced dispersed growth of *Streptomyces* in liquid medium

After germination of the spore, the multicellular bacteria form successively primary and secondary mycelia. In the absence of prophage, the *S. ambofaciens* DSM 40497 tends to form particularly large and dense pellets in response to metabolic stress encountered in BM medium (nitrogen unbalance, translation inhibition, basic pH). Under the same conditions, phage production by *S. ambofaciens* ATCC 23877 is correlated with dispersed growth in sparse clumps and filaments. We propose that phage-induced cell death within the secondary mycelium leads to a dislocation of multicellular aggregates. The subsequent increase in the number of small colonies promotes strain dispersal under stressful conditions.

Figure 1

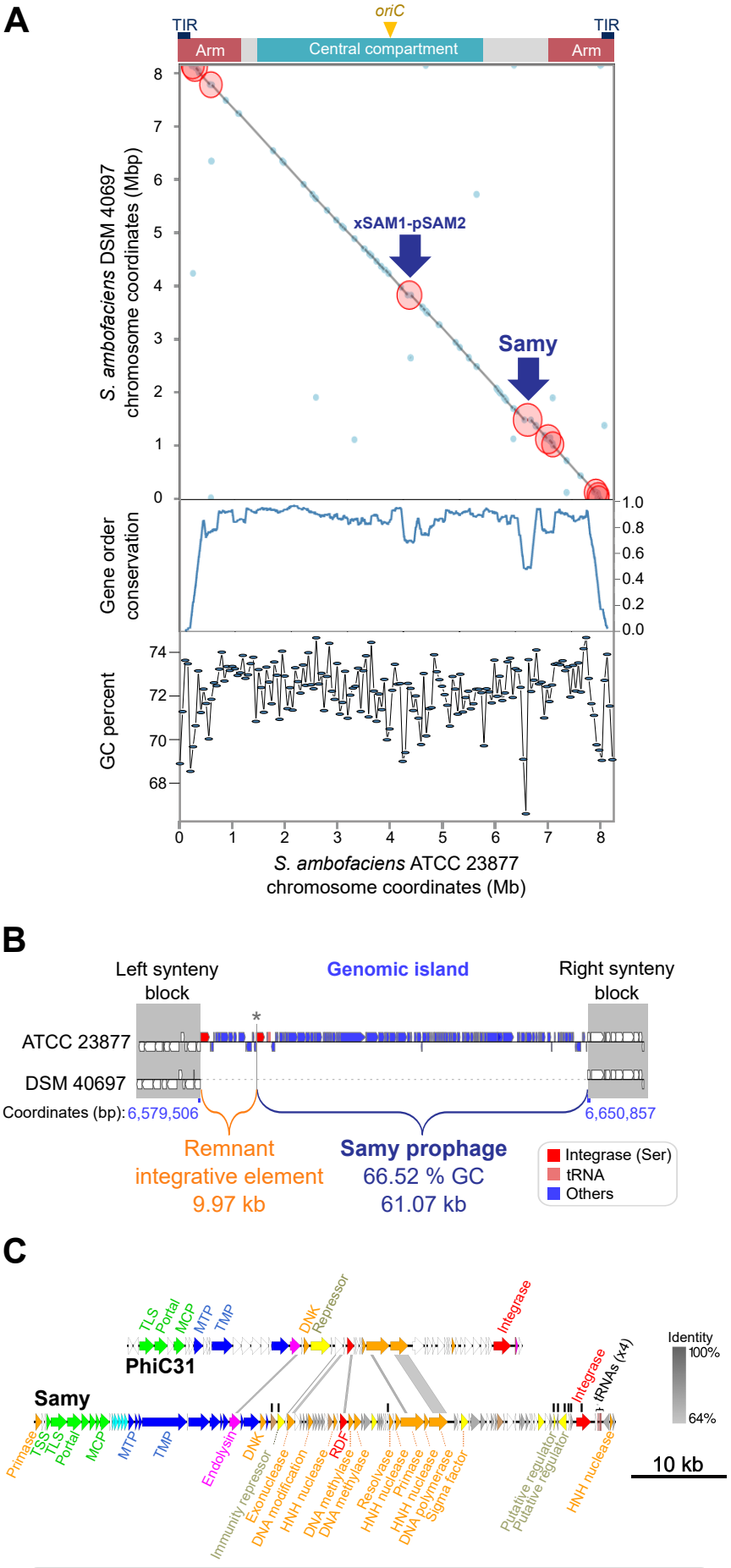

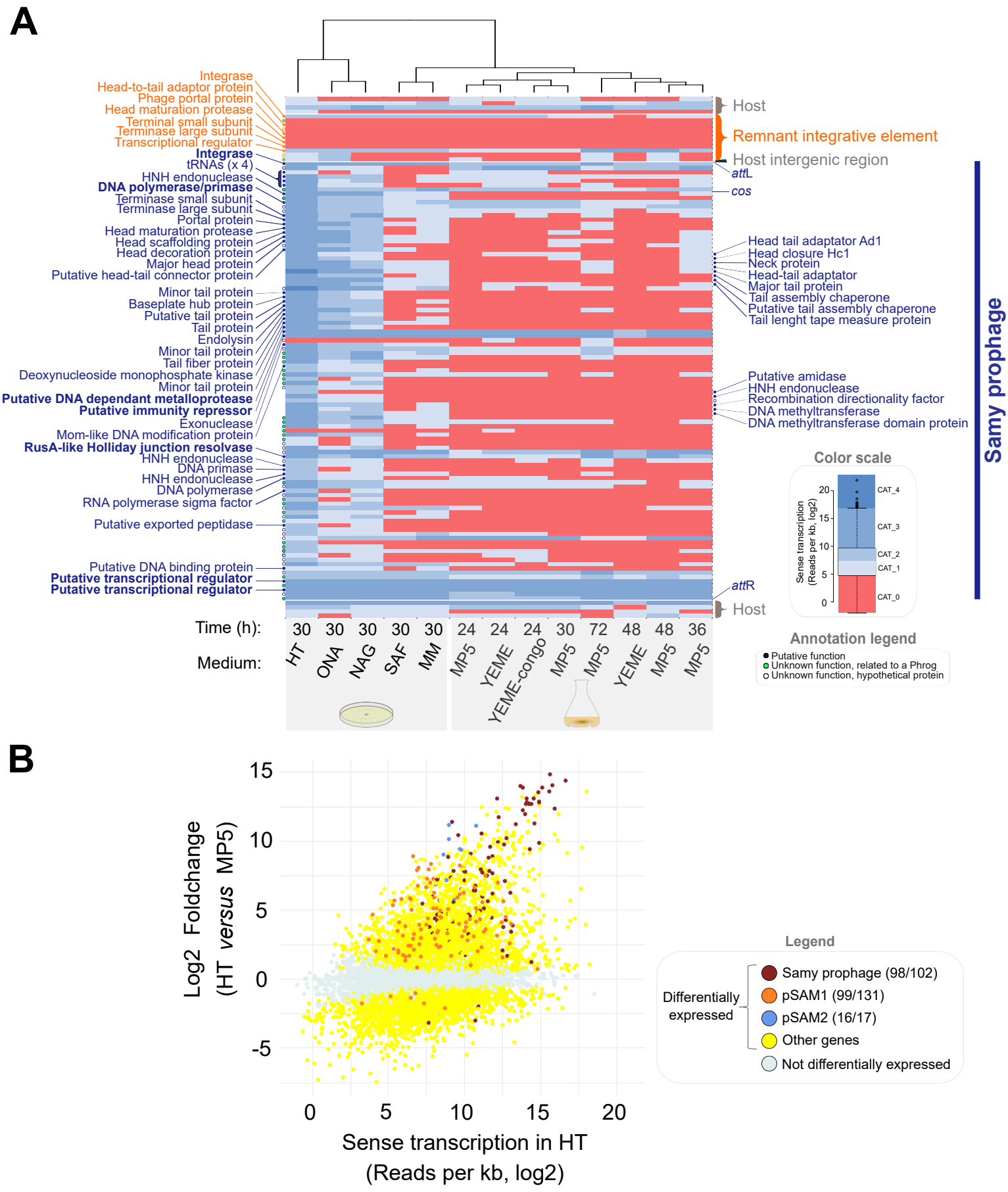

Figure 3

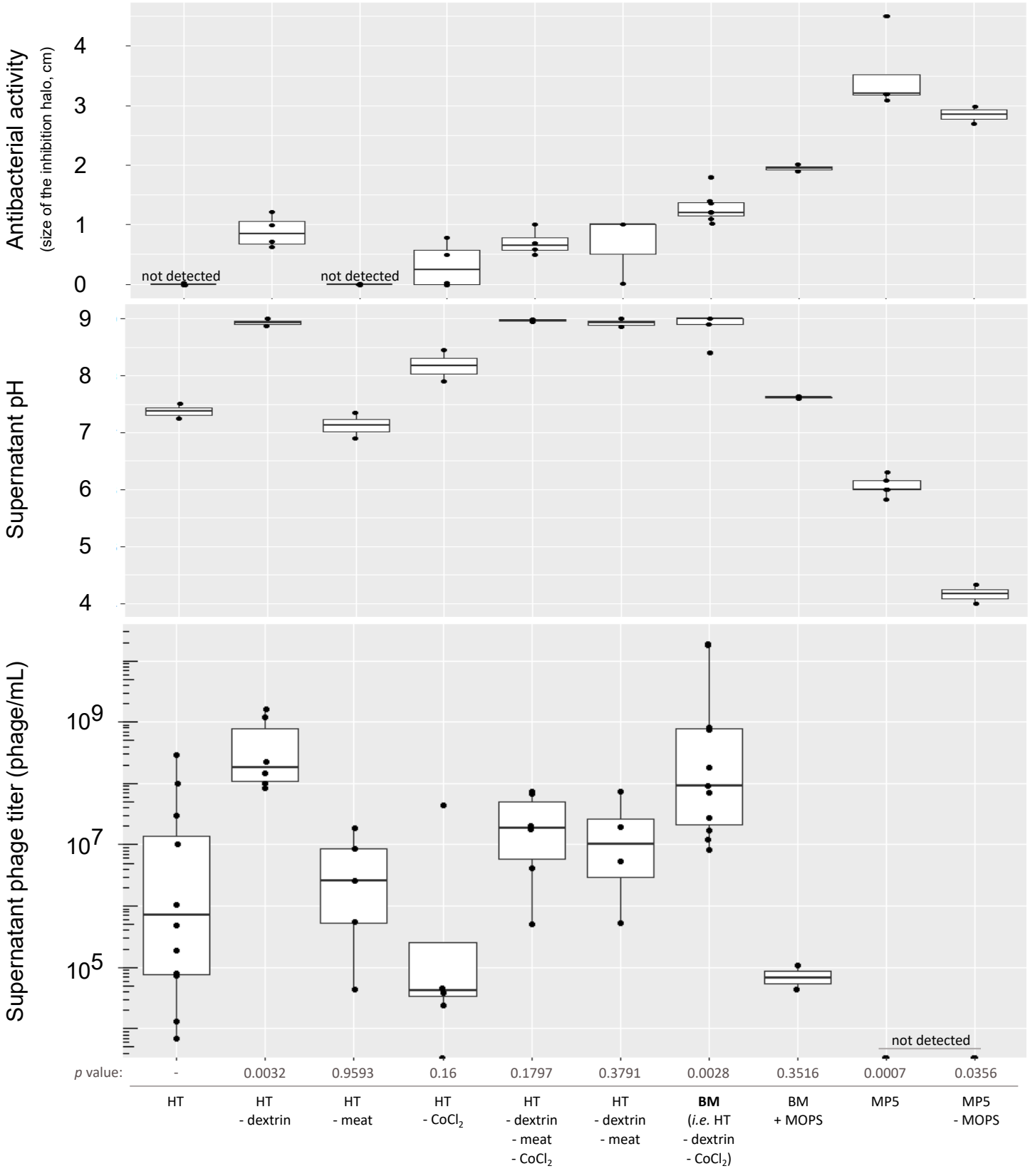

Figure 4

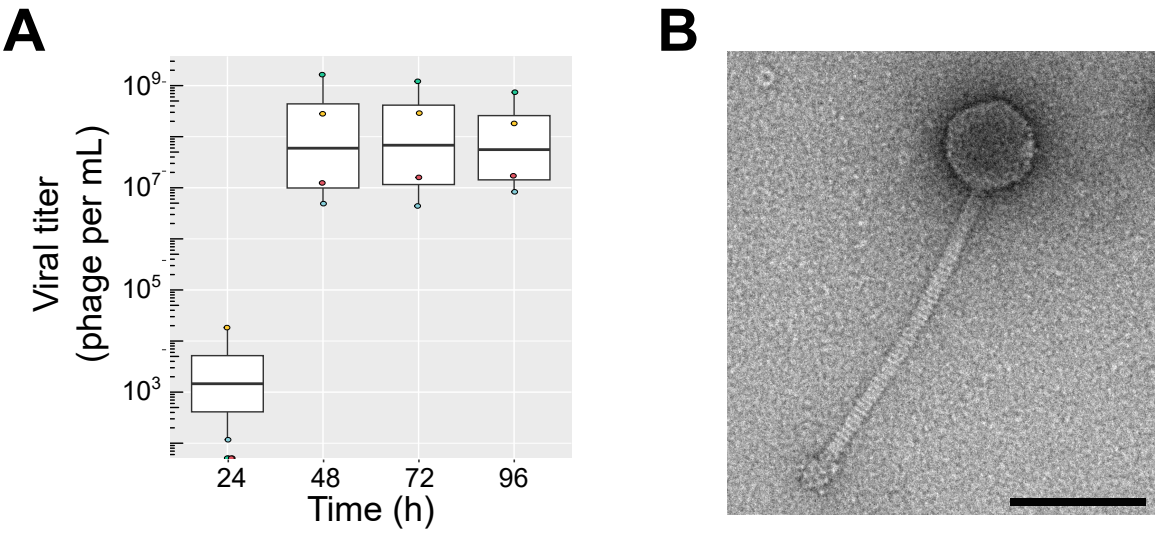

Figure 5

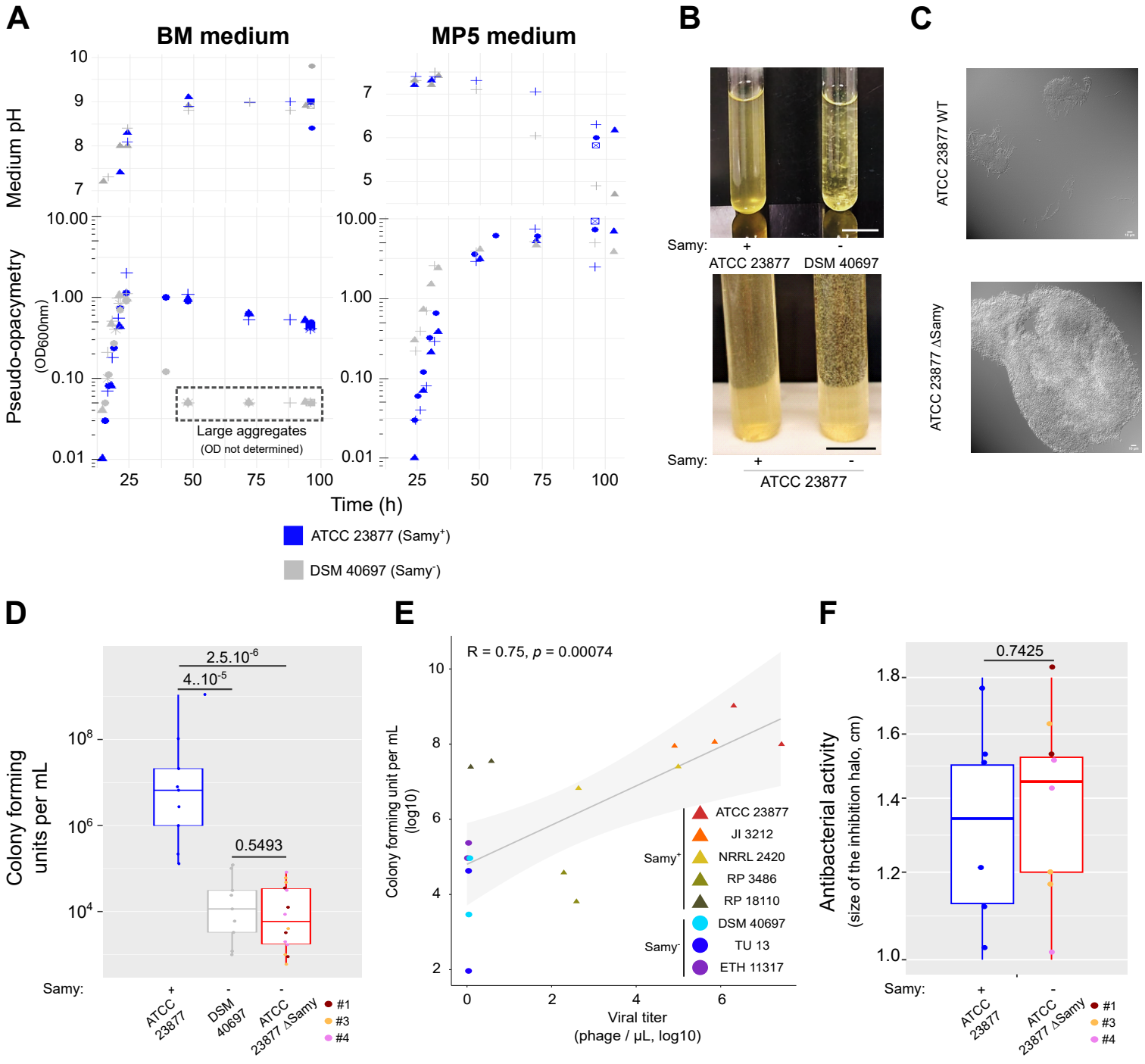

Figure 6

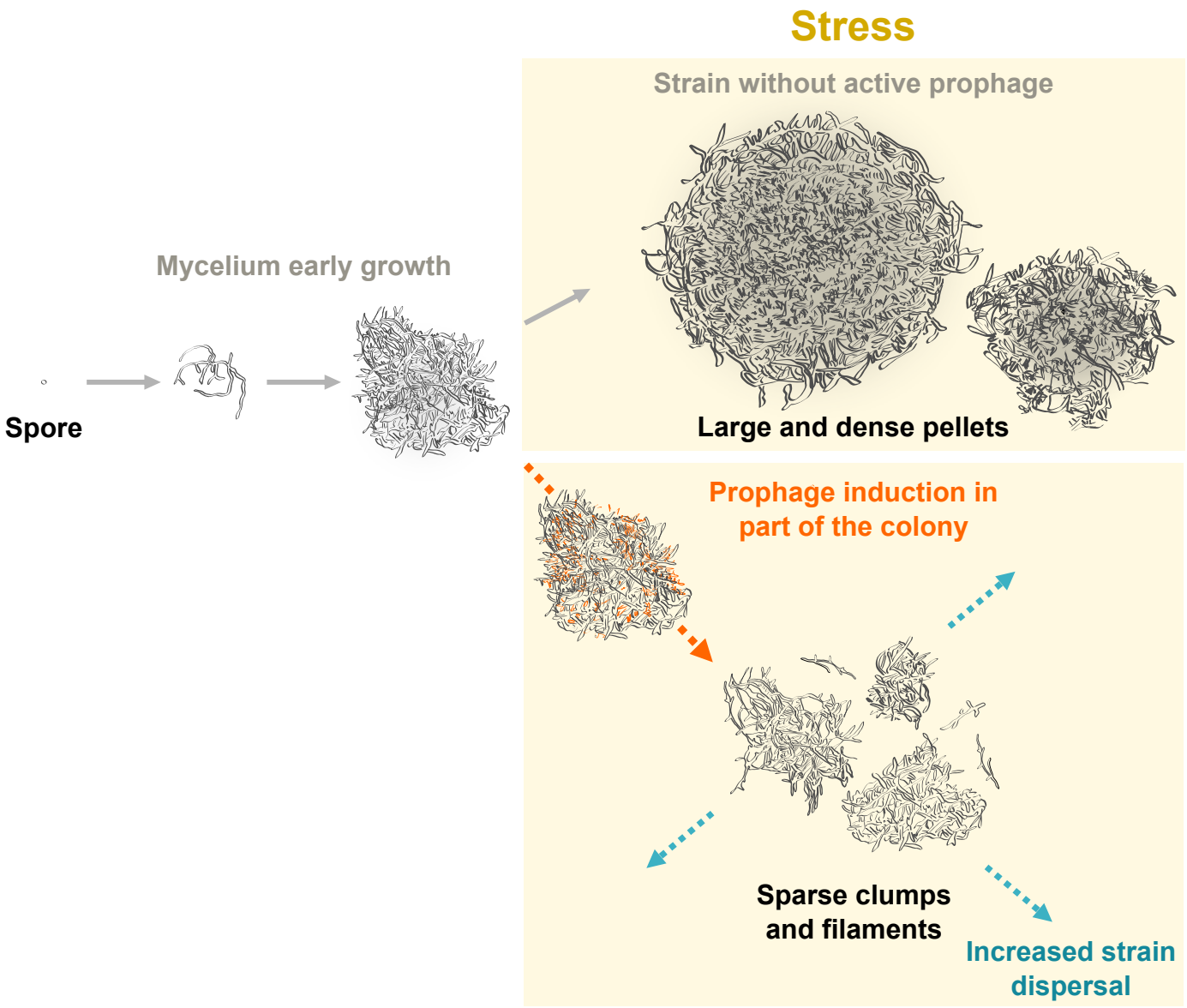

Graphical summary